

Dynamical mean-field theory of electron-phonon interaction in correlated electron materials: general results and application to doped Mott insulators

Andreas Deppeler¹ and Andrew J. Millis²

¹*Center for Materials Theory, Department of Physics and Astronomy, Rutgers University, Piscataway, New Jersey 08854*

²*Department of Physics, Columbia University, 538 W 120th St, New York, New York 10027*

(October 29, 2018)

The dynamical mean-field method is used to formulate a computationally tractable theory of electron-phonon interactions in systems with arbitrary *local* electron-electron interactions in the physically relevant adiabatic limit of phonon frequency small compared to electron bandwidth or interaction scale. As applications, the phonon contribution to the effective mass of a carrier in a lightly doped Mott insulator is determined and the phase separation boundary is discussed.

71.38.-k, 71.27.+a, 71.38.Cn

‘Correlated electron’ materials such as doped Mott insulators [1], high-temperature superconductors [2], heavy fermions [3], and ‘half-metallic’ oxides [4] are central to present-day condensed matter physics because they exhibit many properties that seem incompatible with predictions of the standard paradigm [local density approximation (LDA) band theory plus Boltzmann transport] of metal physics. A crucial role is played by electron-electron interaction effects beyond the scope of the LDA, and theoretical attention has focused on these effects neglecting other physics. However, the electron-phonon interaction is present in all real materials, and it is therefore important to understand its effects in correlated systems. The relevance of electron-lattice effects in the CMR manganites is by now well established [4,5]. Lanzara and co-workers presented photoemission data which, they argue, indicate that electron-phonon effects play an important role in high-temperature superconductivity [6]. On the other hand, the apparent absence of electron-phonon effects in the resistivity of high- T_c materials is a long-standing mystery [7].

There is to date no systematic theoretical extension to correlated materials of the successful Migdal-Eliashberg (ME) theory [8], which describes electron-phonon interactions in *weakly correlated* materials. Electron-phonon interactions in one-dimensional systems have been studied by renormalization group methods [9], and recent improvements in numerical techniques have for example allowed the spin-phonon dynamics of insulating quasi-one-dimensional Peierls systems to be determined in considerable detail [10]. Concerning higher-dimensional, metallic systems, Kim and co-workers [11] argued that near a Mott transition a decrease in electron-phonon coupling was compensated by an increase in carrier mass, leading to electron-phonon effects unrenormalized by proximity to the Mott transition. Our results, to be presented below, disagree with this conclusion. Several authors have used direct numerical simulation [e.g., quantum Monte Carlo (QMC) techniques] of models of electrons interacting both with each other and with lattice vibrations

[12–14]. However, the present limitations of memory size and algorithms have restricted these works mainly to the calculation of static properties, especially phase boundaries and transition temperatures and to the ‘antiadiabatic’ limit of phonon frequency comparable to electronic energy scale.

The development of the dynamical mean-field (DMF) method [15] has opened an important avenue for progress, by showing that if (as occurs for the electron-phonon interaction) the momentum dependence of the electron self-energy is negligible then a good approximation to the correlation physics can be obtained from the solution of a numerically tractable quantum impurity problem plus a self-consistency condition. Unfortunately the straightforward inclusion of the electron-phonon coupling in the DMF formalism is difficult because the mismatch between the typical phonon frequency scale $\omega_0 \lesssim 0.1$ eV and electron energy scale $t \gtrsim 1$ eV renders conventional numerical approaches to the impurity problem prohibitively expensive, except in the ‘antiadiabatic’ limit [14] of relevance to rather few materials. In this paper we present a practical implementation of an adiabatic expansion of the DMF formalism and show how it may be used to determine the phonon contribution to electronic properties of correlated systems. The work reported here builds on previous papers, which introduced the adiabatic expansion [16] and applied it to models involving only electron-lattice interactions [17,18]. As an application we answer the long-standing question of the electron-phonon contribution to the carrier self-energy in a lightly doped Mott insulator. Our methods may easily be extended, e.g., to heavy fermion materials and may be combined with recent extensions of the DMF method [19,20].

We consider the single-site DMF approximation to a general Hamiltonian of the form $H = H_{\text{band}} + H_{\text{el-el}} + H_{\text{ph}} + H_{\text{el-ph}}$, where H_{band} and $H_{\text{el-el}}$ describe electrons moving in some band structure and interacting via some local interaction. We model the phonons as dispersionless quantum oscillators with instantaneous displacement

q^a , mass M_a , and spring constant K_a :

$$H_{\text{ph}} = \frac{1}{2} \sum_{i a} [M_a (\partial_\tau q^a)_i^2 + K_a q_i^{a2}]. \quad (1)$$

Dispersion may be approximately included by treating M, K as Brillouin-zone averages of phonon dispersions or via the more sophisticated techniques of Refs. [21] and [22]. Anharmonic terms such as those considered in Ref. [23] can be easily added and will be seen to be generated.

The electron-phonon coupling is again taken to be local. It is cumbersome to write in general. We illustrate the issues via the physically relevant example of the pseudocubic manganese perovskites. Here the relevant electrons are e_g -symmetry Mn-O hybrid states. The generalized phonon field q_a encompasses (i) a ‘breathing’ mode (symmetric distortion of the Mn-O₆ octahedron) coupling via a constant g_B to the total on-site charge density and (ii) a one-parameter family of Jahn-Teller modes (even-parity, volume-preserving distortions of the Mn-O₆ octahedron) coupling via a matrix element g_{JT} to appropriate differences of occupancy between different orbitals (for a more detailed discussion of the couplings and notation see, e.g. Ref. [5]). These two distortions will be labeled by a scalar coordinate x and a two-component vector $\vec{Q} = (Q_x, 0, Q_z)$, respectively. The coupling term reads (repeated indices are summed)

$$H_{\text{el-ph}} = \sum_i [g_B x_i (n_i - n) + g_{\text{JT}} \vec{Q}_i \cdot c_{i\alpha\beta}^\dagger \vec{\tau}^{ab} c_{ib\beta}], \quad (2)$$

where $\vec{\tau} = (\tau_x, \tau_y, \tau_z)$ are Pauli matrices acting in orbital space, $n_i = \sum_{\alpha\alpha} c_{i\alpha\alpha}^\dagger c_{i\alpha\alpha}$ is the local electron density, and $\langle x_i \rangle = 0$ is defined to be the equilibrium phonon state for a uniform distribution of electrons.

Within the single-site DMF approximation [15] the properties of H may be obtained from the solution of an impurity model specified by the action $S[c, \bar{c}, q, a] = S_0[q] + S_1[c, \bar{c}, q, a]$, with $S_0[q] = 1/(2T) \sum_k q_k^a (K_a + M_a \omega_k^2) q_{-k}^a$ and $S_1[c, \bar{c}, q, a] = S_{\text{el-el}}[c, \bar{c}] + S_{\text{el-ph}}[c, \bar{c}, q] - \sum_{\alpha, n} \bar{c}_{\alpha n} c_{\alpha n} a_n$. Here the terms $S_{\text{el-el}}$ and $S_{\text{el-ph}}$ are obtained in the usual way from the interaction terms listed above, and S is a functional of a mean-field function a , which may depend on spin and orbital indices and expresses the effect of the rest of the lattice upon the single site. It is fixed by equating the impurity Green function $G_{\text{imp}}[a]_n = \delta \ln Z[a] / \delta a_n$ to the local Green function $G_{\text{loc}}[a]_n = \int d^3p / (2\pi)^3 (i\omega_n + \mu - \Sigma[a]_n - H_{\text{band}})^{-1}$ with $\Sigma[a]_n = a_n - G_{\text{imp}}[a]_n^{-1}$. The fields c, \bar{c} and q represent local electronic and phonon degrees of freedom and have been Fourier transformed according to $q(\tau) = \sum_k \exp(-i\omega_k \tau) q_k$ etc. We will index bosonic Matsubara frequencies $\omega_k = 2k\pi T$ by integers k and fermionic Matsubara frequencies $\omega_n = (2n+1)\pi T$ by integers n , i.e., $q_k \equiv q(i\omega_k)$ and $a_n^{-1} \equiv a_\alpha^{-1}(i\omega_n)$.

To analyze the effect of phonons on electronic physics [16,17] we integrate out the electron fields and work with

an effective action $S[q, a] = S_0[q] + S_1[q, a]$, which we expand about the values \bar{q} that extremize S . We introduce an electronic bandwidth or interaction scale t and define the parameters

$$\lambda = \frac{g^2}{Kt}, \quad \gamma = \frac{(K/M)^{1/2}}{t} = \frac{\omega_0}{t}. \quad (3)$$

Crucial objects in the expansion are the vertices

$$\Gamma_N[a]_{k_1, \dots, k_N} = -\frac{1}{(N-1)!} \frac{\delta S_1[q, a]}{\delta q_{k_1}^{a_1} \dots \delta q_{k_N}^{a_N}}, \quad (4)$$

which are connected correlation functions of the electrons-only theory. The adiabatic parameter γ controls the expansion because each phonon loop involves a sum over frequencies of order $\omega_0 \sim \gamma t$ while the vertices Γ vary with frequency on the scale t . If terms of order $\gamma^{3/2}$ and higher are neglected, the $\Gamma_{N>4}$ may be dropped and $\Gamma_{3,4}$ may be approximated by their static value computed using a at $\gamma = 0$. With suitably rescaled fields and frequencies (for details see Ref. [16]) we may write

$$\begin{aligned} S[q, a] = & \frac{1}{2} \sum_k q_k D_k^{-1} q_{-k} \\ & - \frac{\lambda^{3/2} \gamma^{1/2} T^{1/2}}{3} \Gamma_3[a] \sum_{k_1, k_2} q_{k_1} q_{k_2} q_{-k_1-k_2} \\ & - \frac{\lambda^2 \gamma T}{4} \Gamma_4[a] \sum_{k_1, k_2, k_3} q_{k_1} q_{k_2} q_{k_3} q_{-k_1-k_2-k_3}, \end{aligned} \quad (5)$$

where D_k is the phonon propagator, equal for scalar phonons to $1/(1 + \omega_k^2/\omega_0^2 - \lambda \Gamma_2[a]_{k, -k})$, renormalized by electron-electron interaction effects contained in Γ_2 . Note that $\mathcal{O}(\gamma)$ corrections to a , as well as the leading frequency dependence, must be included in Γ_2 .

We used the Hirsch-Fye [24] algorithms distributed with Ref. [15] and routines to compute the connected correlation functions for a single-band Hubbard model. Computations were performed on a Sun workstation; the longest computation Γ_2 at larger U took ~ 40 minutes. Errors (estimated by comparison to exact solution and scaling with system sizes) were less than 2% for parameters shown. Fig. 1 shows that near half filling and for scalar phonons the Hubbard- U strongly decreases Γ_2 , thereby suppressing the polaronic instability occurring at $\lambda \Gamma_2 = 1$. Although the polaronic instability is suppressed a phase separation instability is found for $\lambda \gtrsim 1$ and n near 1; details will be presented elsewhere. For comparison and to demonstrate the power of the method we also present in the right-hand panel results for a model of ‘colossal magnetoresistance’ manganites in which orbitally degenerate electrons are coupled to Jahn-Teller (JT) phonons via the second term in Eq. (2) and also feel both a Hubbard- U and a ‘double-exchange’ interaction arising from a strong coupling to core spins (i.e., the

model defined in Ref. [5] but with a Hubbard- U added). The U is seen to enhance the effect of JT phonons. Fig. 2 shows that for the Hubbard model Γ_3 and Γ_4 are even more rapidly suppressed by U so repulsive interactions effectively decouple electrons from scalar phonons.

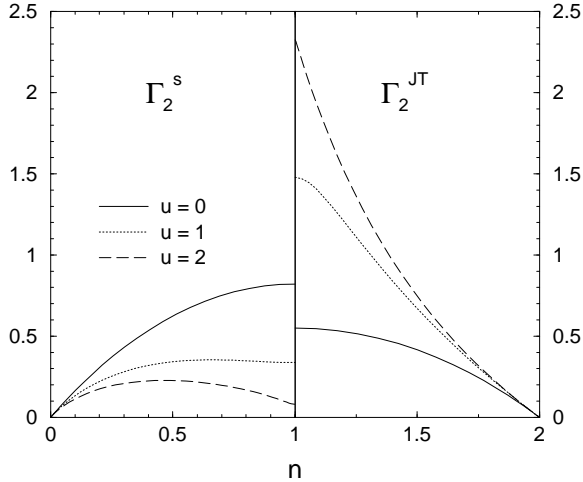


FIG. 1. Left panel: quadratic vertex Γ_2 for scalar phonons as a function of electron density n , for various values of electron-electron interaction $u := U/(2t)$ and $\beta = 10$. Right panel: Γ_2 for Jahn-Teller phonons in the paramagnetic (i.e., *spin-disordered*) phase of the Hubbard-double-exchange model $H_{\text{el-el}} = Un(n-1) + J\vec{S} \cdot \vec{\sigma}$ with $J \rightarrow \infty$. Numerical method: QMC with $L = 32$ time slices.

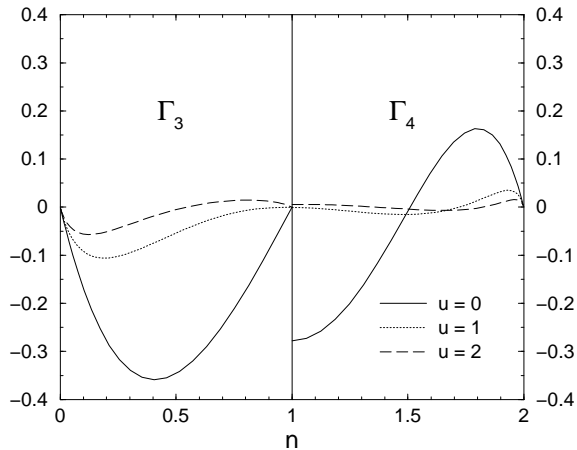


FIG. 2. Left panel: cubic vertex Γ_3 for single-band Hubbard model at $\beta = 10$, with u and electron density n as shown. Right panel: quartic vertex Γ_4 for same parameters. Numerical method: exact enumeration with $L = 16$. Note: $\beta = 10$ is higher than the critical endpoint of the Mott transition occurring at $u \approx 1.5$.

We now turn to the electron self-energy Σ^{ph} due to interactions with phonons, assuming that the effective vertices Γ_N have been determined as discussed above. The calculation is simplified and made more physically

transparent if the action is viewed as a functional of the full electron propagator G rather than as a functional of a . The key object is then the ‘local Luttinger-Ward functional’ $\phi[G]$ defined [25] as the sum of all vacuum-to-vacuum skeleton diagrams and related to the self-energy via $\Sigma = \delta\phi[G]/\delta G$. Within DMF theory, ϕ may be found from the local thermodynamic potential $\Omega_{\text{imp}} = -T \ln Z$ (see Refs. [15] and [26]) so may be computed by an adiabatic expansion. We find $\phi[G] = \phi^{\text{el-el}}[G] + \phi^{\text{ph}}[G] + \mathcal{O}(\gamma^{3/2})$ with $\phi^{\text{ph}}[G] = \frac{1}{2} \sum_k \ln D_k^{-1}$. Therefore

$$\Sigma_n^{\text{ph}} = -\frac{\lambda}{2} \sum_k D_k \frac{\delta\Gamma_2[G]_{k,-k}}{\delta G_n} + \mathcal{O}(\gamma^2). \quad (6)$$

In general Γ_2 and thus $\delta\Gamma_2/\delta G$ vary on the scale of t so $\Sigma^{\text{ph}} \sim \gamma$, an unimportant correction to the bare frequency or electron-electron contribution. However, if $\delta\Gamma/\delta G$ is singular at low frequencies, as in Fermi liquids, then $\partial\Sigma/\partial\omega$ may be of order unity. To investigate this we note that $\Gamma_2[G]_{k,-k} = -2tT \sum_n G_n G_{n+k} (1 + 2tT \sum_{n'} \Lambda_{nn'+k}^R G_{n'} G_{n'+k})$, where the particle-hole *reducible* vertex Λ^R is given in terms of the particle-hole *irreducible* vertex Λ^I via the Dyson equation shown in Fig. 3.

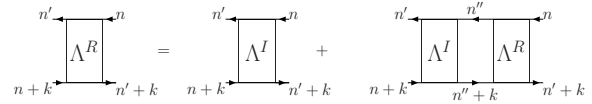


FIG. 3. Diagrammatic Dyson equation connecting the reducible and irreducible particle-hole vertices Λ^R and Λ^I , respectively.

The standard analysis implies that Λ^I is a smooth function of its arguments, so the required singular behavior can only occur if we differentiate on one of the explicit G factors. Further, to $\mathcal{O}(\gamma)$ we may neglect the frequency dependence of the vertices leading to

$$\Sigma_n^{\text{ph}} = \lambda t T \sum_k D_k G_{n+k} \Lambda^2 + \Sigma_n^{\text{ph reg}} \quad (7)$$

with $\Sigma_n^{\text{ph reg}}$ varying with ω_n on the scale of t and

$$\Lambda = 1 + 2tT \sum_n \Lambda_{0n0}^R G_n^2 + \mathcal{O}(\gamma). \quad (8)$$

If the ground state is a Fermi liquid then $G(i\nu) = -i\pi \text{sign}(\nu)\rho(\mu) + G^{\text{inc}}$, where G^{inc} is nonsingular at small frequencies [27]. The leading contribution in γ to m^*/m is then $m^*/m|_{\text{ph}} = 1 + \bar{\lambda}t\rho(\mu)\Lambda^2 + \mathcal{O}(\gamma)$, where $\bar{\lambda} = \lambda/(1 - \lambda\Gamma_2)$.

Λ is a vertex function of the underlying electron-electron theory, determined in general by solving the vertex equation shown in Fig. 3. However, to the order to which we work it is simpler to note that in a Fermi liquid the leading low-frequency behavior of the density-density correlation function is $\chi(\omega) = \chi(0) + iA|\omega|$ with

$A = \Lambda^2 \partial \chi^0 / \partial \omega$ and $\chi_k^0 = -2tT \sum_n G_n G_{n+k}$ is the function obtained by convolving two exact Green functions with no vertex corrections. Thus

$$\Lambda^2 = \frac{\partial \chi_k / \partial (i\omega_k)|_{k=0}}{\partial \chi_k^0 / \partial (i\omega_k)|_{k=0}}. \quad (9)$$

The right hand side of Eq. (9) can be calculated numerically by QMC in the time domain because the leading long-time behavior comes from the first frequency derivative and is $\chi(0 \ll \tau \ll \beta) = (\pi/\beta) \partial \chi_k / \partial (i\omega_k)|_{k=0} / \sin^2(\pi\tau/\beta)$. For $\beta \gtrsim 4$ we find $\chi(\tau)/\chi^0(\tau)$ is very flat in the center region of the interval $(0, \beta)$ (see inset to Fig. 4). The rapid decrease of Λ again shows that the electron-phonon mass enhancement and scattering rate are ‘turned off’ near half filling and for strong correlations, in disagreement with the authors of Ref. [11] who found a weaker decrease in the matrix element, which was moreover cancelled by an increase in effective mass.

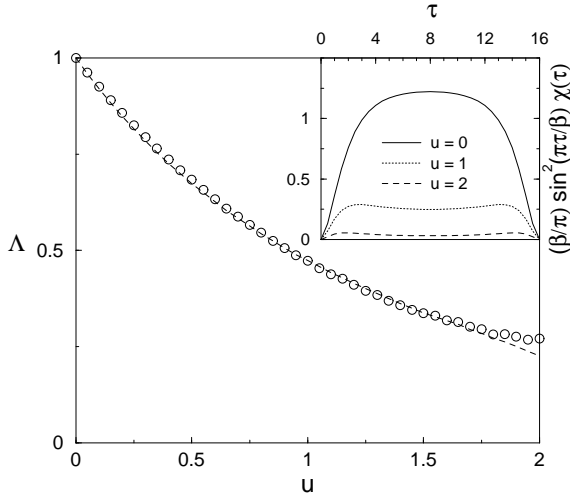


FIG. 4. Static particle-hole scattering renormalization factor as function of $u := U/(2t)$. Numerical results for $\beta = 16$ and $\mu = 0$. Circles: data as described in text. Dashed line: analytic weak-coupling approximation. Inset: imaginary time dependence of χ showing accuracy of approximation.

We summarize the main results of this paper. We have studied a general electron-phonon model in a new approach that combines the adiabatic expansion in $\gamma \ll 1$ of the conventional Migdal-Eliashberg theory with a dynamical mean-field treatment of electron correlations. Our main finding is an effective phonon action correct to $\mathcal{O}(\gamma^{3/2})$ with static coefficients Γ_N ($N = 2, 3, 4$) and vertex Λ , which are easy to compute numerically for various models. For the Holstein-Hubbard model we have shown that the electron-phonon coupling is strongly suppressed by Hubbard- U effects in systems near Mott transitions. Extension of our results to other correlated systems such as heavy fermions would be worthwhile.

We thank S. Blawid for useful discussions, H. Monien

and J. Freericks for critical reading of the manuscript, and NSF DMR00081075 and the University of Maryland/Rutgers MRSEC for support.

-
- [1] M. Imada, A. Fujimori, and Y. Tokura, *Rev. Mod. Phys.* **70**, 1039 (1998)
 - [2] J. Orenstein and A. J. Millis, *Science* **288**, 468 (2000)
 - [3] P. A. Lee, T. M. Rice, J. W. Serene, L. J. Sham, and J. W. Wilkins, *Comm. on Cond. Matter Phys.* **12**, 99 (1986)
 - [4] M. B. Salamon and M. Jaime, *Rev. Mod. Phys.* **73**, 583 (2001)
 - [5] A. J. Millis, R. Mueller, and B. I. Shraiman, *Phys. Rev. B* **54**, 5405 (1996)
 - [6] A. Lanzara, P. V. Bogdanov, X. J. Zhou, S. A. Kellar, D. L. Feng, E. D. Lu, T. Yoshida, H. Eisaki, A. Fujimori, K. Kishio, J. I. Shimoyama, T. Noda, S. Uchida, Z. Hussain, and Z. X. Shen, *Nature* **412**, 510 (2001)
 - [7] M. Gurvitch and A. T. Fiory, *Phys. Rev. Lett.* **59**, 1337 (1987)
 - [8] A. B. Migdal, *Sov. Phys. JETP* **7**, 996 (1958); G. M. Eliashberg, *Sov. Phys. JETP* **11**, 696 (1960)
 - [9] C. Bourbonnais and L. G. Caron, *J. de Physique* **50**, 2751 (1989)
 - [10] S. Trebst, N. Elstner, and H. Monien, *Europhys. Lett.* **56**, 268 (2001)
 - [11] J. H. Kim, K. Levin, R. Wentzcovitch, and A. Auerbach, *Phys. Rev. B* **40**, 11378 (1989)
 - [12] C.-H. Pao and H.-B. Schüttler, *Phys. Rev. B* **60**, 1283 (1999)
 - [13] E. Berger, P. Valásek, and W. von der Linden, *Phys. Rev. B* **52**, 4806 (1995)
 - [14] J. K. Freericks, M. Jarrell, and D. J. Scalapino, *Phys. Rev. B* **48**, 6302 (1993)
 - [15] A. Georges, G. Kotliar, W. Krauth, and M. J. Rozenberg, *Rev. Mod. Phys.* **68**, 13 (1996)
 - [16] A. Deppeler and A. J. Millis, *Phys. Rev. B* **65**, 100301 (2002)
 - [17] S. Blawid and A. J. Millis, *Phys. Rev. B* **63**, 115114 (2001)
 - [18] A. Deppeler and A. J. Millis, cond-mat/0111489
 - [19] V. I. Anisimov, A. I. Poteryaev, M. A. Korotin, A. O. Anokhin, and G. Kotliar, *J. Phys.: Condens. Matter* **9**, 7359 (1997)
 - [20] K. Held, I. A. Nekrasov, N. Blümer, V. I. Anisimov, and D. Vollhardt, *Int. J. Mod. Phys. B* **15**, 2611 (2001)
 - [21] Y. Motome and G. Kotliar, *Phys. Rev. B* **62**, 12800 (2000)
 - [22] M. Jarrell, T. Maier, C. Huscroft, and S. Moukouri, *Phys. Rev. B* **64**, 195130 (2001)
 - [23] J. K. Freericks, V. Zlatić, and M. Jarrell, *Phys. Rev. B* **61**, R838 (2000)
 - [24] J. E. Hirsch and R. M. Fye, *Phys. Rev. Lett.* **56**, 2521 (1986)
 - [25] A. A. Abrikosov, L. P. Gorkov, and I. E. Dzyaloshinski,

Methods of Quantum Field Theory in Statistical Physics
(Dover, 1975)

[26] U. Brandt and C. Mielsch, *Z. Phys.* **82**, 37 (1991)

[27] M. J. Rozenberg, G. Kotliar, and X. Y. Zhang, *Phys. Rev. B* **49**, 10181 (1994)